



Robust Topology Engineering in Multi-Radio Multi-Channel Wireless Networks

Cunqing Hua and Rong Zheng

Department of Computer Science
University of Houston
Houston, TX, 77204, USA
<http://www.cs.uh.edu>

Technical Report Number UH-CS-08-18

January 17, 2009

Keywords: Multi-Radio Multi-Channel wireless networks, robust topology engineering, generalized disjunctive programming, generalized Benders decomposition

Abstract

Topology engineering concerns with the problem of automatic determination of physical layer parameters to generate a network with desired properties. In this paper, we investigate joint power control, channel assignment and radio interface selection for robust provisioning of link bandwidth in infrastructure multi-radio multi-channel(MR-MC) wireless networks in presence of channel variability and external interference. To characterize the logical relationship between spatial contention constraints and power control, we formulate the joint power control and radio-channel assignment as a generalized disjunctive programming problem. The generalized Benders decomposition techniques is applied to decompose the radio-channel assignment (combinatorial constraints) and network resource allocation(continuous constraints) so that the problem can be solved efficiently. The proposed algorithm is guaranteed to converge to the optimal solution within a finite number of iterations. We have evaluated our scheme using traces collected from a wireless mesh testbed and simulation studies in Qualnet. Experiments show that the proposed algorithm is superior to existing schemes in providing larger interference margin, and reducing outage and packet loss probabilities.



Robust Topology Engineering in Multi-Radio Multi-Channel Wireless Networks

Cunqing Hua and Rong Zheng

Abstract

Topology engineering concerns with the problem of automatic determination of physical layer parameters to generate a network with desired properties. In this paper, we investigate joint power control, channel assignment and radio interface selection for robust provisioning of link bandwidth in infrastructure multi-radio multi-channel(MR-MC) wireless networks in presence of channel variability and external interference. To characterize the logical relationship between spatial contention constraints and power control, we formulate the joint power control and radio-channel assignment as a generalized disjunctive programming problem. The generalized Benders decomposition techniques is applied to decompose the radio-channel assignment (combinatorial constraints) and network resource allocation(continuous constraints) so that the problem can be solved efficiently. The proposed algorithm is guaranteed to converge to the optimal solution within a finite number of iterations. We have evaluated our scheme using traces collected from a wireless mesh testbed and simulation studies in Qualnet. Experiments show that the proposed algorithm is superior to existing schemes in providing larger interference margin, and reducing outage and packet loss probabilities.

Index Terms

Multi-Radio Multi-Channel wireless networks, robust topology engineering, generalized disjunctive programming, generalized Benders decomposition

I. INTRODUCTION

Deployment of wireless infrastructure networks (e.g., on-campus WiFi networks, wireless mesh networks in rural communities, WiMax) faces many challenges from the need of regular site survey (“can you hear me now?”) to the difficulty in configuring a plural of system or device parameters to meet end-user requirements. The later issue is further exacerbated by inherent dynamics due to changes in channel condition, environments, user population, and co-existing networks. While online adaptation of configurations in face of such dynamics is desirable from performance optimization perspective, its practice in real systems shall be taken with some cautions for two reasons. First, collection of state information required for adaptation are often delayed and incomplete. Second, significant protocol overhead is incurred in collecting these information and reconfigure the system. Furthermore, in extreme cases, instability may ensue if adaption is performed too frequently. Consequently, as been demonstrated by current Internet practice, adaption of network configurations is often limited to local domain or infrequently on a network scale. This motives us to design *robust* solutions that may not be optimized for the current state but continue to perform *well* in presence of moderate degree of network dynamics.

In this paper, we address the problem of robust topology engineering in infrastructure wireless networks. Topology engineering is defined as *automatic determination of physical layer parameters to generate a network with the desired properties*. Compared to topology control, a well-studied problem in ad hoc networks, topology engineering is more general in that the objective is not limited to network connectivity [17]–[19], [21], [31] or interference reduction [10], [29], [30], rather the traffic-carrying operational aspect of a network such as provisioning of link bandwidth based on *a priori* knowledge of link (cell)-level demands. Robustness of a topology engineering solution is quantified by “interference margin”, a notion first proposed by Hua *et al.* [13]. Generally speaking, interference margin reflects the allowance toward fluctuating link condition and unmanageable interferences while sustaining desired level of quality of service.

With the decreasing cost and increasing programmability of wireless devices, many tunable parameters are now at our disposal in topology engineering. In this paper, we consider the choice of transmission power, channel assignment and radio interface in multi-radio multi-channel(MR-MC) wireless networks. Finding a robust set of parameters to meet link bandwidth requirements is non-trivial. First, spatial contention relation between links is no longer fixed, instead, it depends on transmit power levels. This makes it hard to incorporate power control and

spatial contention constraints in a single optimization framework. Second, the optimization problem involves the radio-channel assignment (combinatorial constraints), and network resource limitation (continuous constraints). It belongs to the mixed-integer nonlinear programming (MINLP) problems, which is known to be NP-hard in general [24]. In this paper, we overcome these barriers by exploiting the specific structure of the problem at hand, and by introducing additional variables and constraints. To decouple spatial contention constraint from the power control, we introduce disjunctive sets to characterize the logical relation of power control and spatial contention between links, which can be relaxed and expressed as a set of linear constraints. To address the MINLP problem, the generalized Benders decomposition technique [11] is applied to decompose the optimization problem to a primal problem and a master problem. The primal problem is obtained by fixing the binary variables from the original problem, and the master problem is obtained via nonlinear duality theory for the solution of binary variables. The proposed algorithm is guaranteed to converge to the optimal solution within a finite number of iterations.

Using traces collected from a wireless mesh testbed, we conduct a set of experiments to evaluate the performance of the proposed topology engineering solution and compare it with other existing schemes. We also incorporate the trace data in the Qualnet simulator [26] and compare the performance of several algorithms through simulation study. The experiments show that the proposed algorithm is superior to existing schemes in providing larger interference margin, and reducing outage and packet loss probability in presence of channel variability. We also demonstrate the convergence behavior of the proposed algorithm.

Main contribution: In this paper, we make the following contributions.

- Incorporation of bandwidth requirements in topology engineering in MR-MC wireless networks.
- A new power control, channel assignment and radio interface assignment scheme is designed with several advantageous features: i) incorporating measurement-driven interference and link capacity model; ii) robustness to external interference and fluctuation of channel, and iii) provable convergence to global optimality.

The rest of this paper is organized as follows. In Section III, we provide a categorization of existing work. The models assumed and the problem statement are formally defined in Section IV. The solution based on generalized Benders decomposition technique is presented in Section V. Evaluation using real-world trace data from our mesh testbed and simulation is presented in Section VI. Finally, we conclude the paper with future research avenue in Section VII.

II. BACKGROUND AND RELATED WORK

Topology control in multihop wireless networks is a topic received much attention in the research community. The primary goal of topology control is “to determine the transmit power level of each node so as to maintain network connectivity, mitigate interference, improve spatial reuse, while consuming the minimum possible power” [10]. The work in [17]–[19], [21], [31] deal with the selection of common or heterogeneous power to maintain connectivity. The impact of interference based on physical model has been addressed in [10], [29], [30]. In this paper, we deliberately avoid using the term “topology control” because of two salient differences from existing work. First, almost all existing topology control scheme limits themselves to networks with a single channel, single radio interface per node. This greatly limits the ability to mitigate interference and increase capacity. Second, we view topology not just as *reachability* among nodes but also *how well* they are connected and *how much bandwidth* can be sustained between pairs of nodes in presence of transmission activity in other part of the network. This is the reason the term “topology engineering” is introduced.

Many channel assignment schemes have been proposed in literature. They can be roughly categorized as, traffic-agnostic [14], [28] vs traffic-aware [13], [24], [25], assuming binary [3], [15], [24], [25] vs physical interference and link capacity model [14], centralized [3], [15], [24], [25] and distributed schemes [14], [28]. A more detailed survey of channel allocation schemes can be found in [13].

Very little work addresses the issue of *joint* channel allocation and power control in infrastructure wireless networks. Leveraging the prior work on power control, user association [20], and channel assignment [14], Broustis *et al.* [5] design measurement-driven guidelines (MDG) for the combination of the three functions to improve the overall network capacity in dense WLANs. It has been shown that intelligent frequency allocation across APs, load-balancing of user affiliations across APs, and adaptive power-control for each AP shall be done in sequence based on the current operational conditions such as existence of overlapping APs or non-cooperative APs. In [9], Foschini and Miljanic proposed heuristic for joint autonomous channel assignment and channel allocation in cellular

networks. The authors assume each base station is associated a pre-determined set of orthogonal channels. Based on use arrival process, the algorithm determines which channel among the set of orthogonal channels and power levels to be used for uplink and downlink communication. Though the proposed heuristic is fully distributed, due to its online nature, global optimality cannot be achieved. Digham [8] proposed a centralized joint power and channel allocation in a single cell cognitive radio network. Three constraints are imposed, namely, i) total power constraint among all users, ii) channel constraint (no two user can use the same channel) and iii) interference constraints to primary users. In our formulation, we impose per radio power constraint and allow sharing of the same channel among users in TDD fashion.

III. WIRELESS NETWORK MODELS

A. Overview

The MR-MC wireless networks considered in this paper can be modeled as a directed and connected graph $\mathcal{G} = (\mathcal{N}, \mathcal{L})$, where a link l is in \mathcal{L} if and only if: (i) the transmitter of the link can communicate with the receiver directly; (ii) a positive link bandwidth requirement D_l is associated with link l .

Each node $n \in \mathcal{N}$ has R_n radios, each radio can switch between Q orthogonal channels. We assume $R_n \leq Q$ since it is not useful to operate multiple radios on the same channel simultaneously. If the number of incident links of a node is larger than the number of its radios, some of its radios will be shared by multiple links. All radios are assumed to be *half-duplex*, so if multiple links are assigned to the same radio, they should be scheduled to transmit at different time since only one link can be served by the radio at each time.

We assume that each wireless interface has *per-link* power control capability, that is, if multiple links are assigned to the same radio, the radio can operate at different power levels for different links. Without loss of generality, each radio is assumed to be limited by a minimum power level P_{min} and a maximum power level P_{max} .

Each link l is associated with a unique pair of radios at the transmitter and the receiver, and a single channel. This formulation can be extended to the case when multiple radios are used concurrently to support the demand between a pair of transmitter and receiver nodes by introducing multiple logical links. To characterize the assignment of radios and channel for a link l , and its spatial contention relation with other links, we define four binary variables as follows,

- x_l^i : equals 1 if radio i is assigned to link l at the transmitter node, and 0 otherwise.
- y_l^j : equals 1 if radio j is assigned to link l at the receiver node, and 0 otherwise.
- u_l^q : equals 1 if channel q is assigned to link l , and 0 otherwise.
- v_l^k : equals 1 if link l is contended by link k over the same channel, and 0 otherwise.

Since each link can only use one transmitting radio and one receiving radio, and one channel at each time, the following constraints should hold for any feasible radio and channel assignment solution,

$$\sum_{i \in R_{s_l}} x_l^i = 1, \sum_{j \in R_{t_l}} y_l^j = 1, \text{ and } \sum_{q \in Q} u_l^q = 1, \forall l \in \mathcal{L} \quad (1)$$

In the following, without abusing the notations, let x, y, u and v denote the multisets of elements $\{x_l^i\}, \{y_l^j\}, \{u_l^q\}, \{v_l^k\}$ respectively for $i \in R_{s_l}, j \in R_{t_l}, q \in Q$ and $l, k \in \mathcal{L}$, where s_l and t_l denote the transmitter and receiver of link l .

B. Interference margin and effective link capacity

We consider the generalized physical interference model whereby all concurrent transmissions are treated as interference to a link l when the transmitter of the link is transmitting to its intended receiver. In this model, the signal-to-interference-plus-noise ratio (SINR) at the receiver is given by

$$SINR_l = \frac{P_l G_{ll}}{N_0 + I_e + I_c} \quad (2)$$

where P_l is the transmit power allocated to link l , G_{kl} is the channel gain from the transmitter of link k to the receiver of link l , N_0 is noise power. The perceived interference at the receiver consists of two terms, I_e is the external interference from non-manageable devices or networks (e.g., o-existing WLANs, WPANs and other EMI sources), and I_c is the interference from the concurrent transmissions within the same networks. In particular, the

concurrent interference I_c can be given by $I_c = \sum_{k \neq l} P_k G_{kl}$, which depends on the location of all concurrent transmissions to the receiver nodes. Here we make a *conservative* approximation and assume that I_c is dominated by the strongest concurrent transmission. The most *conservative* scenario occurs when the interfering node is on the extended line of the link locating in the opposite direction of the transmitter. In this case, the concurrent interference can be approximated as $I_c \approx P_{max} G_{cl}$, where G_{cl} is the channel gain from interfering node to the receiver, assuming the node transmits with maximum power level.

Two sources of variability exist in deployed networks. First, the channel gain between the transmitter and receiver is subject to large-scale and small-scale fading due to signal attenuation over distance, shadowing, and multipath effects etc. The second are external interferences from devices operating in overlapping or adjacent spectrum bands. The variations of channel gain and external interferences are generally unmanageable, and the interference level is difficult to predict.

To capture these effects, the *interference margin* concept was introduced in [13] as a quantitative measure to characterize robustness to channel and external interference variability, where the *interference margin* σ_l is defined for each link l to represent the *maximum channel and external interference variability that can be tolerated to sustain the targeted transmission rate* for the link. We can re-write the effective SINR as a function of the link transmit power, *mean* channel gain and the *interference margin* as

$$\overline{SINR}_l = \frac{P_l \bar{G}_{ll}}{N_0 + I_c + \sigma_l} \quad (3)$$

where the mean channel gain \bar{G}_{ll} can be obtained from measurement data.

Let the effective link capacity B_l of link l is a function of the effective SINR, or $B_l = f(\overline{SINR}_l)$. For example, for Gaussian broadcast channel, the effective link capacity is found to be bounded by

$$B_l \leq B \log \left(\frac{P_l \bar{G}_{ll}}{N_0 + I_c + \sigma_l} \right), \forall l \in \mathcal{L}. \quad (4)$$

where B is the channel bandwidth in hertz. The interference margin should be chosen to ensure $\overline{SINR}_l \geq \gamma$ such that a target link capacity is achievable.

To understand the physical meaning of interference margin, let us consider the case where the worst-case realization of channel gain G_{ll} is bounded by $(1 - \Delta)G_{ll}$. It is easy to show that as long as $\sigma_l \geq \frac{I_c + \Delta(N_0 + I_c)}{1 - \Delta}$, the target link capacity can be attained.

C. Power control and spatial contention constraints

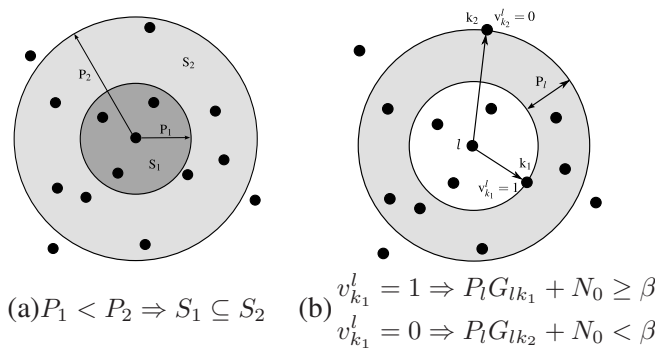


Fig. 1. Transmission power vs. spatial contention domain

Representation of contention relations among wireless links depends on many factors, including the transmit power, topological relation, and the contention model. In this paper, we adopt the *transmitter-based* contention model after the *carrier sensing* mechanism used in IEEE 802.11 MAC. Note the contention relation is asymmetric in general. Specifically, we assume that a link l is contending with a link k if only if the perceived power level at

Details are omitted due to space limit.

the transmitter of link k is higher than a certain threshold β when link l is transmitting. That is, if $P_l G_{lk} + N_0 \geq \beta$, we say link l is contending with link k ; otherwise if $P_l G_{lk} + N_0 < \beta$, link l is not contending with link k .

The *contending domain* S_l of a link l is defined as the set of links with which link l contends, or equivalently, $S_l = \{k : P_l G_{lk} + N_0 \geq \beta\}$. Clearly, S_l depends on link l 's transmit power level. For instance, as shown in Fig. 1(a), the contending domain S_1 with lower transmit power level P_1 is a subset of the contending domain S_2 with higher transmit power level P_2 . Thus, it is non-trivial to model power control and spatial contention constraints in a single optimization framework.

To address this problem, we introduce an indicator variable v_k^l to characterize the contention relation between links l and k . That is, $v_k^l = 1$ iff link l is contending with link k , or $P_l G_{lk} + N_0 \geq \beta$; or else $v_k^l = 0$, which implies $P_l G_{lk} + N_0 < \beta$. The feasible region of P_l can then be determined by the value of v_k^l . For example, in Fig. 1(b), $v_{k_1}^l = 1$ and $v_{k_2}^l = 0$, which limits the feasible region of P_l to the gray area.

The logical relation of v_k^l and P_l can be captured by disjunctive sets, consisting of two disjunctions separated by the or(\vee) operator and negation(\neg) operator:

$$\left[P_l G_{lk} + N_0 \geq \beta \right] \vee \left[P_l G_{lk} + N_0 < \beta, \neg v_k^l \right] \quad (5)$$

which can be understood as a logical expression enforcing only one set of constraint based on the value of v_k^l .

Note that the degree of freedom of v_k^l 's is limited. They are subject to several constraints:

- **Minimum and maximum power constraint:** If $P_{min} G_{lk} + N_0 \geq \beta$, then $v_k^l \equiv 1$. That is, if the received power at the transmitter of link k is sufficiently large even when the transmitter of link l is using the minimum power level, then v_k^l should always equal to one. Similarly, $v_k^l \equiv 0$ if $P_{max} G_{lk} + N_0 < \beta$.
- **Symmetry constraint** should be imposed to guarantee that contention relationship is symmetric, namely, $v_k^l = v_l^k$. Kawadia [21] and Kauffmann2007 [14] have both argued the need for symmetric carrier sensing and packet reception for better performance.
- **Spatial dependency** is due to the spatial correlation among links. Consider the scenario with three links k_1, k_2 and l as shown in Fig. 1(b), G_{lk_1} and G_{lk_2} denote the channel gain between l and k_1, k_2 respectively. Without loss of generality, assuming $G_{lk_1} \leq G_{lk_2}$, or $P_l G_{lk_1} \leq P_l G_{lk_2}$. This implies (i) if $v_{k_1}^l = 1$, then $P_l G_{lk_2} + N_0 > P_l G_{lk_1} + N_0 \geq \beta$. Therefore, $v_{k_2}^l = 1$; (ii) if $v_{k_2}^l = 0$, then $v_{k_1}^l$ also equals to 0 since $P_l G_{lk_1} + N_0 \leq P_l G_{lk_2} + N_0 < \beta$. The above relationship can be expressed more compactly as follows:

$$v_{k_1}^l \leq v_{k_2}^l, \forall k_1, k_2, l, \text{ iff } G_{lk_1} < G_{lk_2}. \quad (6)$$

D. Radio and channel constraints

To characterize the contention relationship in wireless networks, we adopt the set of constraints in line with maximal scheduling [6], [32], which yields simple distributed scheduling similar to the IEEE 802.11 DCF. The formulation can be readily extended to other forms of contention characterization such as that using clique constraints.

Let \mathcal{L}_l^s and \mathcal{L}_l^r denote the set of links sharing the same transmitter and receiver with link l , respectively; and $\mathcal{L}_l^c = \mathcal{L} \setminus (\mathcal{L}_l^s \cup \mathcal{L}_l^r)$ denotes the set of links that may interfere with link l (including link l itself). Consider contention from all links sharing the same radios or channel, the aggregate time required to satisfy the demand of link l (operating in radio i, j and channel q) and that of all its contending links is bounded by,

$$T_l = \sum_{k \in \mathcal{L}_l^s} \frac{x_k^i D_k}{B_k} + \sum_{k \in \mathcal{L}_l^r} \frac{y_k^j D_k}{B_k} + \sum_{k \in \mathcal{L}_l^c} \frac{u_k^q v_l^k D_k}{B_k}, \quad (7)$$

where D_k/B_k is the time to satisfy the traffic demand of link k . T_l is a function of (x, y, u, v) and (σ, P) . In the worst case, all contending links form a clique and should be scheduled at different time. Therefore, it is required that

$$T_l(x, y, u, v, \sigma, P) \leq 1, \forall l \in \mathcal{L}. \quad (8)$$

The RHS of the above inequality can be replaced by a factor κ ($\kappa \geq 1$) to reflect the looseness of maximal scheduling constraints resulting in a tighter capacity region. However, schedulability is not always guaranteed when $\kappa > 1$.

IV. ROBUST POWER CONTROL AND CHANNEL ASSIGNMENT

A. Problem formulation

In robust topology engineering, the goal is to determine a set of transmit power, radio-channel assignment for all links such that the link bandwidth remain satisfied in presence of moderate channel dynamics. Intuitively, the larger the interference margin, the more robust the resulting power and radio-channel assignment to channel variability and external interferences. To this end, we define a utility function U_l for each link l , which is a function of the *interference margin* σ_l . It has the following properties: (i) the utility function $U_l(\sigma_l)$ is monotonic increasing, strictly concave and 2nd order differentiable; (ii) $U_l(\sigma_l)$ is additive so that the aggregated utility of all links is $\sum_{l \in \mathcal{L}} U_l(\sigma_l)$. Different utility functions have been defined for different fairness models, such as proportional fairness and max-min fairness [23].

The robust power control and radio-channel assignment problem can be formally stated as a network utility maximization problem with the constraints specified by (1), (5), (6) and (8) as follows:

$$\begin{aligned}
 & \max \quad \sum_{l \in \mathcal{L}} U_l(\sigma_l) \\
 & \text{s.t.} \quad T_l(x, y, u, v, \sigma, P) \leq 1, \forall l \in \mathcal{L}, \\
 & \quad \left[P_l G_{lk} + N_0 \geq \beta \right] \bigvee \left[P_l G_{lk} + N_0 < \beta \right], \forall l, k \in \mathcal{L} \\
 & \quad v_{k_1}^l \leq v_{k_2}^l, \forall k_1, k_2, l, G_{lk_1} < G_{lk_2}. \\
 & \quad v_l^k = v_k^l, \forall k, l \in \mathcal{L} \\
 & \quad \sum_{i \in R_{s_l}} x_l^i = 1, \sum_{j \in R_{t_l}} y_l^j = 1, \sum_{q \in Q} u_l^q = 1, \forall l \in \mathcal{L}, \\
 & \quad x_l^i, y_l^j, u_l^q, v_l^k = \{0, 1\}, \forall l \in \mathcal{L}, \\
 & \quad P_{min} \leq P_l \leq P_{max}, \forall l \in \mathcal{L}, \\
 & \quad \sigma_l \geq 0, \forall l \in \mathcal{L}
 \end{aligned} \tag{9}$$

This problem belongs to the generalized disjunctive program(GDP) problem [2], where the discrete choices of spatial contention relations are represented by Boolean variables v_k^l in the forms of disjunctions. This GDP problem can be transformed to a mixed-integer nonlinear programming problem using relaxation techniques discussed in the following subsections.

B. Relaxation of disjunctive set

There are several ways to relax the disjunctive set (5), such as the *big-M formulation*, the *Beaumont surrogate* and the *convex hull relaxation* [2]. Depending on the property of the disjunctive set, there is a trade-off between the tightness of the relaxation and the complexity. The disjunctive set in (5) is a *proper* set because the intersection of the feasible region of all disjunctions is empty. In this case, the *big-M formulation* is as tight as other two relaxation techniques, but with much lower complexity. Therefore we choose the *big-M formulation* to relax the disjunctive set (5) with the following constraints:

$$\begin{aligned}
 \beta - P_l G_{lk} - N_0 & \leq M_1(1 - v_k^l) \\
 P_l G_{lk} + N_0 - \beta & \leq M_2 v_k^l
 \end{aligned} \tag{10}$$

where M_1 and M_2 are two sufficiently large valid upper bounds for P_l obtained as follows ,

$$\begin{aligned}
 M_1 & = \max\{\beta - P_l G_{lk} - N_0 | P_{min} < P_l \leq P_{max}\} \\
 & = \beta - P_{min} G_{lk} - N_0
 \end{aligned} \tag{11}$$

and

$$\begin{aligned}
 M_2 & = \max\{P_l G_{lk} + N_0 - \beta | P_{min} < P_l \leq P_{max}\} \\
 & = P_{max} G_{lk} + N_0 - \beta
 \end{aligned} \tag{12}$$

respectively.

Substituting (11) and (12) into (10), and re-arranging the equations, we can obtain

$$m_l^k \leq P_l \leq M_l^k, \forall l, k \in \mathcal{L}. \quad (13)$$

where

$$\begin{aligned} m_l^k &= [P_{\min} G_{lk}(1 - v_k^l) + (\beta - N_0)v_k^l]/G_{lk} \\ M_l^k &= [P_{\max} G_{lk}v_k^l + (\beta - N_0)(1 - v_k^l)]/G_{lk} \end{aligned}$$

Eq.(13) suggests that the transmit power P_l is constrained by a set of lower and upper bounds determined by the contention indicator variable v_k^l s. A compact form of the feasible region for P_l can be derived as follows,

$$\max_{k \in \mathcal{L}} \{m_l^k\} \leq P_l \leq \min_{k \in \mathcal{L}} \{M_l^k\}, \forall l \in \mathcal{L}. \quad (14)$$

Note that if $v_k^l = 0$, we have $m_l^k = P_{\min}$ and $M_l^k = (\beta - N_0)/G_{lk}$; otherwise, if $v_k^l = 1$, we have $m_l^k = (\beta - N_0)/G_{lk}$ and $M_l^k = P_{\max}$. This implies that the constraint $P_l \in [P_{\min}, P_{\max}]$ is redundant and can be incorporated into (14).

C. Relaxation of product variables

The radio and channel constraint in (7) includes a binary product $u_k^q \cdot v_l^k$. We introduce an auxiliary variable $z_l^{k,q} = u_k^q \cdot v_l^k$. Clearly, $z_l^{k,q}$ can only be 0 or 1 depending on the values of u_k^q and v_l^k , and their relation is bounded by following linear constraints [22]

- If $u_k^q = 0$ or $v_l^k = 0$, then $z_l^{k,q} = 0$. This is equivalent to the following linear constraint

$$-u_k^q - v_l^k + 2z_l^{k,q} \leq 0 \quad (15)$$

- If $u_k^q = 1$ and $v_l^k = 1$ then $z_l^{k,q} = 1$. This is equivalent to the following linear constraint

$$u_k^q + v_l^k - z_l^{k,q} \leq 1 \quad (16)$$

Therefore, the radio and channel constraint can be rewritten as

$$\begin{cases} T_l(x, y, z, \sigma, P) \\ = \sum_{k \in \mathcal{L}_l^s} \frac{x_k^i D_k}{B_k} + \sum_{k \in \mathcal{L}_l^i} \frac{y_k^j D_k}{B_k} + \sum_{k \in \mathcal{L}_l^c} \frac{z_l^{k,q} D_k}{B_k} \leq 1 \\ -u_k^q - v_l^k + 2z_l^{k,q} \leq 0, \forall k \in \mathcal{L}, \\ u_k^q + v_l^k - z_l^{k,q} \leq 1, \forall k \in \mathcal{L}. \end{cases} \quad (17)$$

D. Convex approximation of the effective link capacity

In general, the effect link capacity is not a concave function of the transmit power and interference margin variables. However, for the Gaussian broadcast channel, the effective link capacity B_l is known to be upper bounded by Shannon's capacity formula as $B_l = B \log(1 + \text{SINR}_l)$. When the SINR is relatively higher, we can use the approximation $\log(1+x) \approx \log(x)$ and introduce the log variable for P_l and σ_l applying the geometric programming techniques [4], that is, $P_l = \log(P)$, $\tilde{\sigma}_l = \log(\sigma_l)$. The effective link capacity B_l can be re-written as

$$B_l \approx B \log\left(\frac{e^{\tilde{P}_l} \tilde{G}_l}{N_0 + e^{\tilde{\sigma}_l}}\right) = -B \log\left(\frac{N_0}{\tilde{G}_l} e^{-\tilde{P}_l} + \frac{1}{\tilde{G}_l} e^{\tilde{\sigma}_l - \tilde{P}_l}\right) \quad (18)$$

Thus the effective link capacity B_l is a concave function of the variables \tilde{P}_l and $\tilde{\sigma}_l$ since "log-sum-exp" expressions are convex [4].

E. Problem transformation

Applying the big-M relaxation (14) to the disjunctive sets, the binary linearization (17) to the product of binary variables, and the convex approximation of effective link capacity(18), we transform the GDP form of the problem defined in (9) to mixed integer nonlinear programming (MINLP) problem as follows,

$$\begin{aligned}
\max \quad & \sum_{l \in \mathcal{L}} U_l(\tilde{\sigma}_l) \\
\text{s.t.} \quad & T_l(x, y, z, \tilde{\sigma}, \tilde{P}) \leq 1, \forall l \in \mathcal{L}, \\
& -u_k^q - v_l^k + 2z_l^{k,q} \leq 0, \forall l, k \in \mathcal{L}, \\
& u_k^q + v_l^k - z_l^{k,q} \leq 1, \forall l, k \in \mathcal{L}, \\
& v_{k_1}^l \leq v_{k_2}^l, \forall k_1, k_2, l, G_{lk_1} < G_{lk_2}, \\
& v_l^k = v_k^l, \forall k, l \in \mathcal{L}, \\
& \sum_{i \in R_{s_l}} x_l^i = 1, \sum_{j \in R_{t_l}} y_l^j = 1, \sum_{q \in Q} u_l^q = 1, \forall l \in \mathcal{L}, \\
& x_l^i, y_l^j, u_l^q, v_l^k, z_l^{k,q} = \{0, 1\}, \forall l \in \mathcal{L}, \\
& \max_{k \in \mathcal{L}} \{m_l^k\} \leq e^{\tilde{P}_l} \leq \min_{k \in \mathcal{L}} \{M_l^k\}, \forall l \in \mathcal{L},
\end{aligned} \tag{19}$$

where (x, y, u, v, z) are a set of binary variables, $\tilde{\sigma}$ and \tilde{P} are a set of continuous variables.

V. GENERALIZED BENDERS DECOMPOSITION SOLUTION

In general, the MINLP problems is known to be NP-hard problems and no efficient solutions exist because the complexity may increase exponentially with problem size. However, the MINLP problem in (19) has a special property in that it is convex with respect to continuous variables if the discrete variables are fixed. The generalized Benders decomposition (GBD) [11] has been proposed for MINLP problem with this property. In a recent work [13], GBD technique has been applied for solving the channel assignment problem with similar structure.

The basic idea of the GBD algorithm is to decompose the original MINLP problem to a *primal* problem and a *master* problem and solve them iteratively. The *primal* problem corresponds to the original problem with fixed binary variables, solving this problem provides the information about the *lower* bound and the Lagrange multipliers corresponding to the constraints. The *master* problem is derived through nonlinear duality theory using the Lagrange multipliers obtained from the primal problem. The solution to the master problem gives the information about the *upper* bound as well as the binary variables that can be used for primal problem in next iteration.

A. Primal problem

In the following, for the easy of exposure, let $\Omega := (x, y, z, u, v)$ represent the set of binary variables, and $\hat{\Omega}$ denotes the binary variables with specific values in $\{0, 1\}$.

The primal problem of the MINLP problem in (19) is obtained by fixing the binary variables to $\hat{\Omega}$:

$$\mathcal{P}(\hat{\Omega}) \left\{ \begin{array}{l} f(\hat{\Omega}) = \max \sum_{l \in \mathcal{L}} U_l(\tilde{\sigma}_l) \\ \text{s.t.} \quad T_l(\hat{\Omega}, \tilde{\sigma}, \tilde{P}) \leq 1, \forall l \in \mathcal{L}, \\ \max_{k \in \mathcal{L}} \{m_l^k\} \leq e^{\tilde{P}_l} \leq \min_{k \in \mathcal{L}} \{M_l^k\}, \forall l \in \mathcal{L}, \\ \tilde{\sigma}_l \geq 0, \forall l \in \mathcal{L}. \end{array} \right. \tag{20}$$

where $f(\hat{\Omega})$ is the value function of the primal problem. Since the optimal solution of this problem is also a feasible solution to problem (19), the optimal value $f(\hat{\Omega})$ provides a lower bound to the original problem.

In general, not all choices of binary variables lead to a feasible primal problem. It should be treated differently depending on whether the primal problem is feasible or not:

- **Feasible Primal**

If the primal problem is feasible, we form the *partial Lagrangian* for the primal problem by introducing Lagrange multipliers $\lambda \in \mathcal{R}^{\mathcal{L}}$ only for the constraints $T_l(\hat{\Omega}, \tilde{\sigma}, \tilde{P}) \leq 1, \forall l \in \mathcal{L}$. Namely,

$$L(\hat{\Omega}, \tilde{\sigma}, \tilde{P}, \lambda) = \sum_{l \in \mathcal{L}} U_l(\tilde{\sigma}_l) + \sum_{l \in \mathcal{L}} \lambda_l \left(1 - T_l(\hat{\Omega}, \tilde{\sigma}, \tilde{P})\right) \tag{21}$$

The objective function of the dual problem is defined as

$$V(\lambda) = \sup_{\tilde{\sigma}, \tilde{P}} \left\{ L(\hat{\Omega}, \tilde{\sigma}, \tilde{P}, \lambda) \mid \begin{array}{l} \max_{k \in \mathcal{L}} \{m_l^k\} \leq e^{\tilde{P}_l} \leq \min_{k \in \mathcal{L}} \{M_l^k\}, \\ \tilde{\sigma}_l \geq 0, \forall l \in \mathcal{L}. \end{array} \right\} \quad (22)$$

The Lagrange dual problem associated with the feasible primal problem (20) is to solve

$$\begin{array}{ll} \min & V(\lambda) \\ \text{s.t.} & \lambda \succeq 0. \end{array} \quad (23)$$

• Infeasible Primal

If the primal problem is infeasible, we define a set Γ as

$$\Gamma = \{\hat{\Omega} \mid T_l(\hat{\Omega}, \tilde{\sigma}, \tilde{P}) \leq 1, \text{ for some } \tilde{\sigma}, \tilde{P}\}$$

and consider the following feasibility-checking problem

$$\mathcal{F}(\hat{\Omega}) \left\{ \begin{array}{l} g(\hat{\Omega}) = \min_{l \in \mathcal{L}_1} \sum w_l T_l^+(\hat{\Omega}, \tilde{\sigma}, \tilde{P}) \\ \text{s.t.} \quad T_l(\hat{\Omega}, \tilde{\sigma}, \tilde{P}) \leq 1, \forall l \in \mathcal{L}_2. \\ \max_{k \in \mathcal{L}} \{m_l^k\} \leq P_l \leq \min_{k \in \mathcal{L}} \{M_l^k\}, \forall l \in \mathcal{L}. \\ \tilde{\sigma}_l \geq 0, \forall l \in \mathcal{L}. \end{array} \right.$$

where $T_l^+ = \max(0, T_l - 1)$, \mathcal{L}_1 is set of infeasible constraints, \mathcal{L}_2 is the set of feasible constraints, and $\mathcal{L} = \mathcal{L}_1 \cup \mathcal{L}_2$. The weights w_l s are nonnegative and not all zero. In particular, if we let $w_l = 1, l \in \mathcal{L}_1$, it is equivalent to a l_1 -minimization problem. In this case, a *partial Lagrangian* for the infeasible primal problem can be defined by introducing Lagrange multipliers $\mu \in \mathcal{R}^{\mathcal{L}}$ for the constraints as

$$G(\hat{\Omega}, \tilde{\sigma}, \tilde{P}, \mu) = \sum_{l \in \mathcal{L}} \mu_l (T_l(\hat{\Omega}, \tilde{\sigma}, \tilde{P}) - 1) \quad (24)$$

It is shown in [11] that $\hat{\Omega}$ belong to the set Γ if and only if they satisfy the following system:

$$\begin{array}{l} 0 \geq \inf_{\tilde{\sigma}, \tilde{P}} G(\hat{\Omega}, \tilde{\sigma}, \tilde{P}, \mu), \forall \mu \in \Lambda \\ \text{where } \Lambda = \{\mu_l \geq 0, \sum_{l \in \mathcal{L}} \mu_l = 1.\} \end{array} \quad (25)$$

B. Master problem

The original MINLP problem defined in (19) can be written as

$$\begin{array}{l} \max_{\Omega} \sum_{l \in \mathcal{L}} U_l(\tilde{\sigma}_l) = \max_{\Omega} f(\Omega) \\ = \max_{\Omega} (\min_{\lambda} \sup_{\tilde{\sigma}, \tilde{P}} L(\Omega, \tilde{\sigma}, \tilde{P}, \lambda)) \\ = \max \quad \beta \\ \text{s.t.} \quad \beta \leq \sup_{\tilde{\sigma}, \tilde{P}} L(\Omega, \tilde{\sigma}, \tilde{P}, \lambda), \forall \lambda \succeq 0, \\ \Omega \in \{0, 1\} \cap \Gamma. \end{array} \quad (26)$$

where the first equality is obtained from (22) and (23). Incorporating (25) into (26), we can make the constraints over set Γ explicit and obtain the following master problem:

$$\mathcal{M}(\tilde{\sigma}, \tilde{P}, \lambda, \mu) \left\{ \begin{array}{l} \max \quad \beta \\ \text{s.t.} \quad \beta \leq \sup_{\tilde{\sigma}, \tilde{P}} L(\Omega, \tilde{\sigma}, \tilde{P}, \lambda), \forall \lambda_l \geq 0, \\ 0 \geq \inf_{\tilde{\sigma}, \tilde{P}} G(\Omega, \tilde{\sigma}, \tilde{P}, \mu), \forall \mu_l \in \Lambda, \\ -u_k^q - v_l^k + 2z_l^{k,q} \leq 0, \forall l, k \in \mathcal{L}, \\ u_k^q + v_l^k - z_l^{k,q} \leq 1, \forall l, k \in \mathcal{L}, \\ v_{k_1}^l \leq v_{k_2}^l, \forall k_1, k_2, l, G_{lk_1} < G_{lk_2}, \\ v_l^k = v_l^l, \forall k, l \in \mathcal{L}, \\ \sum_{i \in R_{s_l}} x_i^l = 1, \sum_{j \in R_{t_l}} y_l^j = 1, \sum_{q \in Q} u_l^q = 1, \\ \Omega \in \{0, 1\}. \end{array} \right. \quad (27)$$

Note that the master problem has two inner optimization problems as its constraints, which need to be considered for all λ and μ . This implies that the master problem has a very large number of constraints. In [16], following relaxations have been proposed for the first two constraints of master problem at iteration n as

$$\begin{aligned} \beta &\leq \tilde{L}(\Omega^{(i)}, \tilde{\sigma}^{(i)}, \tilde{P}^{(i)}, \lambda^{(i)}), \forall i \in \tilde{\mathcal{P}}^n, \\ 0 &\geq \tilde{G}(\Omega^{(i)}, \tilde{\sigma}^{(i)}, \tilde{P}^{(i)}, \mu^{(i)}), \forall i \in \mathcal{F}^n, \end{aligned} \quad (28)$$

The relaxed constraints at i th iteration ($i \leq n$) are given respectively by

$$\begin{aligned} \tilde{L}(\Omega^{(i)}, \tilde{\sigma}^{(i)}, \tilde{P}^{(i)}, \lambda^{(i)}) &= L(\Omega^{(i)}, \tilde{\sigma}^{(i)}, \tilde{P}^{(i)}, \lambda^{(i)}) \\ &+ \nabla_{\Omega} L(\Omega^{(i)}, \tilde{\sigma}^{(i)}, \tilde{P}^{(i)}, \lambda^{(i)}) (\Omega - \Omega^{(i)}) \end{aligned}$$

and

$$\begin{aligned} \tilde{G}(\Omega^{(i)}, \tilde{\sigma}^{(i)}, \tilde{P}^{(i)}, \mu^{(i)}) &= G(\Omega^{(i)}, \tilde{\sigma}^{(i)}, \tilde{P}^{(i)}, \mu^{(i)}) \\ &+ \nabla_{\Omega} G(\Omega^{(i)}, \tilde{\sigma}^{(i)}, \tilde{P}^{(i)}, \mu^{(i)}) (\Omega - \Omega^{(i)}) \end{aligned}$$

$\tilde{\mathcal{P}}^n$ and \mathcal{F}^n are the set of feasible and infeasible primal problems solved up to iteration n :

$$\begin{aligned} \tilde{\mathcal{P}}^n &:= \{i \leq n : \tilde{\mathcal{P}}(\Omega^{(i)}) \text{ is feasible}\} \\ \mathcal{F}^n &:= \{i \leq n : \mathcal{F}(\Omega^{(i)}) \text{ is infeasible}\} \end{aligned} \quad (29)$$

C. Algorithm

Main procedure: The GBD algorithm is operated in an iterative way as shown in Algorithm 1. In each iteration n , the optimal primal-dual pair $(\tilde{\sigma}^{(n)}, \tilde{P}^{(n)}, \lambda^{(n)})$ (for feasible primal problem) or $(\tilde{\sigma}^{(n)}, \tilde{P}^{(n)}, \mu^{(n)})$ (for infeasible primal problem) are solved with fixed integer variables $\Omega^{(n)}$, which are fed into (27) to solve the relaxed master problem. The relaxed problem provides an upper bound to the master problem and can be used to generate the primal problem in the next iteration, then the same procedure is repeated until converges.

In this procedure, the sequence of upper bounds is non-increasing and the set of lower bounds is nondecreasing, and the domain of the binary variables are finite. The two sequences are proven to converge and the algorithm will stop at the optimal solution $(\Omega^*, \tilde{\sigma}^*, \tilde{P}^*)$ within a finite number of iterations [11], [16].

Algorithm 1: GBD power control and channel assignment algorithm

input : Link-level traffic demand $D_l, \forall l \in \mathcal{L}$.

output: Binary variables Ω , link transmission power P and interference margin σ .

begin

Set $m = 1$ and choose $\Omega^{(n)} \in \{0, 1\}$.

$LB^0 \leftarrow -\infty, UB^0 \leftarrow \infty, \mathcal{P}^0 \leftarrow \emptyset, \mathcal{F}^0 \leftarrow \emptyset$.

while $LG^{n-1} < UB^{n-1}$ **do**

if the primal problem is feasible **then**

 Solve the primal problem $\mathcal{P}(\Omega^{(n)})$ to obtain optimal solution $\tilde{\sigma}^{(n)}, \tilde{P}^{(n)}$ and $\lambda^{(n)}$;

$\mathcal{P}^n \leftarrow \mathcal{P}^{n-1} \cup \{n\}, \mathcal{F}^n \leftarrow \mathcal{F}^{n-1}$;

$LB^n \leftarrow \max(LB^{n-1}, f(\Omega^{(n)}))$;

if $LB^n = f(\Omega^{(n)})$ **then**

$(\Omega^*, \tilde{\sigma}^*, \tilde{P}^*) \leftarrow (\Omega^{(n)}, \tilde{\sigma}^{(n)}, \tilde{P}^{(n)})$;

end

else if the primal problem is infeasible **then**

 Solve the feasibility-check problem $\mathcal{F}(\Omega^{(n)})$ to obtain the optimal solution $\tilde{\sigma}^{(n)}, \tilde{P}^{(n)}$ and $\mu^{(n)}$;

$\mathcal{P}^n \leftarrow \mathcal{P}^n, \mathcal{F}^n \leftarrow \mathcal{F}^{n-1} \cup \{n\}$;

end

 Solve the master problem $\mathcal{M}(\tilde{\sigma}^{(n)}, \tilde{P}^{(n)}, \lambda^{(n)}, \mu^{(n)})$ to obtain the optimal solution $\Omega^{(n+1)}$ and $\beta^{(n)}$;

$UB^n \leftarrow \beta^{(n)}, n \leftarrow n + 1$;

end

return $\Omega^*, \tilde{\sigma}^*$ and \tilde{P}^* .

end

Primal problem: The primal problem can be solved distributively using the dual decomposition technique. Let us consider the feasible primal case, from (17) and (20), we have

$$\begin{aligned}
 L(\hat{\Omega}, \tilde{\sigma}, \tilde{P}, \lambda) &= \sum_{l \in \mathcal{L}} U_l(\tilde{\sigma}_l) + \sum_{l \in \mathcal{L}} \lambda_l \left(1 - T_l(\hat{\Omega}, \tilde{\sigma}, \tilde{P}) \right) \\
 &= \sum_{l \in \mathcal{L}} U_l(\tilde{\sigma}_l) + \sum_{l \in \mathcal{L}} \lambda_l \left(1 - \sum_{k \in \mathcal{L}_l^s} \frac{x_k^i D_k}{B_k} \right. \\
 &\quad \left. - \sum_{k \in \mathcal{L}_l^j} \frac{y_k^j D_k}{B_k} - \sum_{k \in \mathcal{L}_l^c} \frac{z_l^{k,q} D_k}{B_k} \right) \\
 &= \sum_{l \in \mathcal{L}} \left[U_l(\tilde{\sigma}_l) - \gamma_l \frac{D_l}{B_l} \right] + \sum_{l \in \mathcal{L}} \lambda_l
 \end{aligned}$$

where γ_l is the aggregate multipliers of links conflicting with link l over radio and channel, which is given by

$$\gamma_l = \sum_{k \in \mathcal{L}_l^s} \lambda_k x_k^i + \sum_{k \in \mathcal{L}_l^j} \lambda_k y_k^j + \sum_{k \in \mathcal{L}_l^c} \lambda_k z_l^{k,q}$$

Given γ_l , each link l can find $\tilde{\sigma}_l$ and \tilde{P}_l by solving its local Lagrangian function as follows

$$\begin{aligned}
 &(\tilde{\sigma}_l(\gamma_l), \tilde{P}_l(\gamma_l)) \\
 &= \arg \max_{\tilde{\sigma}_l, \tilde{P}_l} \left\{ U_l(\tilde{\sigma}_l) - \gamma_l \frac{D_l}{B_l} \left| \begin{array}{l} \max_{k \in \mathcal{L}} \{m_l^k\} \leq e^{\tilde{P}_l} \leq \min_{k \in \mathcal{L}} \{M_l^k\}, \\ \tilde{\sigma}_l \geq 0, \forall l \in \mathcal{L}. \end{array} \right. \right\}
 \end{aligned}$$

The Lagrangian multipliers can be obtained by solving the following dual problem as

$$\min_{\lambda \geq 0} \sum_{l \in \mathcal{L}} \left[U_l(\tilde{\sigma}_l) - \gamma_l \frac{D_l}{B_l} \right] + \sum_{l \in \mathcal{L}} \lambda_l \tag{30}$$

which can be solved using the following gradient method,

$$\lambda_l = \left[\lambda_l - \alpha (1 - T_l(\hat{\Omega}, \tilde{\sigma}, \tilde{P})) \right]^+ \tag{31}$$

where α is a sufficiently small positive step size, and $[\cdot]^+$ denotes the projection onto the nonnegative orthant.

Algorithm 2: Time Slot Scheduling Algorithm

input : Slot demand n_l and conflicting set $I_l, \forall l \in \mathcal{L}$.
output: Time slot assignment A .
begin
 $t \leftarrow 0$;
while *there exists a link $l \in \mathcal{L}$ with $n_l > 0$* **do**
 $A(t) \leftarrow \emptyset, U(t) \leftarrow \{l | n_l > 0, l \in \mathcal{L}\}$.
while $U(t) \neq \emptyset$ **and** $n_l > 0, \forall l \in U(t)$ **do**
Select a link $l \in U(t)$ and set $l^* \leftarrow \arg \max_{l' \in I_l} n_{l'}$;
 $A(t) \leftarrow A(t) \cup \{l^*\}$;
 $U(t) \leftarrow U(t) \setminus (\{l^*\} \cup I_{l^*})$;
 $n_{l^*} \leftarrow n_{l^*} - 1$;
end
 $t = t + 1$;
end
return A .
end

Master problem: The values of interference margin, transmit power and Lagrangian multiplier obtained from the primal problem by each link need to be reported to a central server (e.g., the gateway nodes in a mesh network) for solving the master problem (27). Note that in each iteration, only the latest information needs to be reported, the communication cost is constant and low. The relaxed master problem is a integer linear programming (ILP) problem, which can be solved using some ILP solvers such as "glpk" [12]. The complexity of solving the master problem can be reduced since it does not need to solve the problem to optimality in each iteration, therefore, some heuristic algorithms can be used to find an integer solution in order to generate an optimality cut, however, the convergence of the procedure may not be guaranteed [7].

D. Scheduling

Given the power, radio and channel assignment results, it remains to decide when a link should be scheduled for packet transmission. We devise a TDMA schedule so that in each time slot only a set of conflict-free links are scheduled for transmission. Let n_l denote the number of slots required by a link l , which is given by $n_l = \lceil D_l / B_l \tau \rceil$, where τ is the slot duration. Let I_l denote the set of links conflicting with link l . For a time slot t , let $A(t)$ denote the set of links assigned in this time slot, and $U(t)$ denote the remaining links yet to be assigned. The scheduling algorithm works as in Algorithm 2.

The above algorithm is essentially a maximal scheduling, where in each time slot, the set of links belonging to a maximal independent set are scheduled. Maximal scheduling yields simple distributed implementations [6], [32].

VI. PERFORMANCE EVALUATION

A. Evaluation setup

In this section, we evaluate the performance of the proposed *robust power* (RP) and radio-channel assignment scheme using measurement traces and simulation. For comparison purpose, other two algorithms have been implemented as baselines

- The FP (fixed power) algorithm uses the radio-channel assignment algorithm proposed in [13] with fixed transmit power for all links.
- The SP (symmetric power) algorithm incorporates the power control scheme in [20] and channel assignment scheme in [14], both using the Gibbs sampler technique. The power control algorithm tries to optimize both transmit power and carrier sense threshold to preserve the symmetry sensing among links.

The received signal strength (RSS) measurements are collected from an indoor testbed (Fig. 2). Each node is an embedded Wireless Router Application Platform (WRAP) board with 233 MHz AMD Geode SC1100 CPU, 64Mb DRAM, with two Mini PCI Atheros 802.11a/b/g wireless cards and one Ethernet port. Multiple rounds of measurements are conducted to build RSS profile for all links. In each round, only one node is scheduled to broadcast 100 UDP packets of 12 bytes payload at the lowest data rate (1Mbps), other nodes can receive the packet

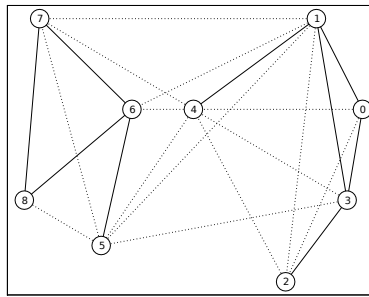


Fig. 2. Testbed topology

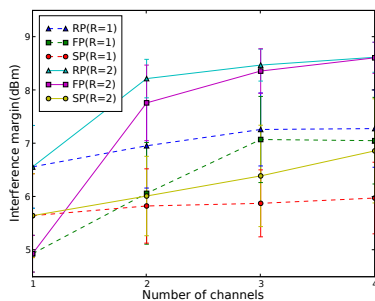


Fig. 3. Interference margin

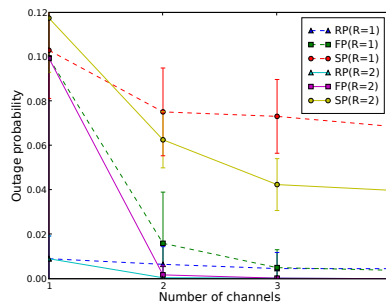


Fig. 4. Outage probability

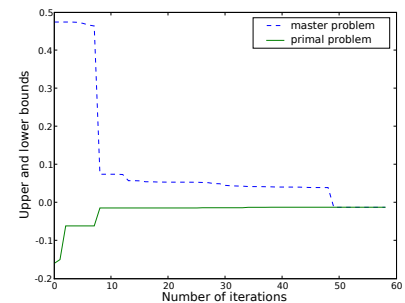


Fig. 5. Convergence

and extract the RSS information from the received packet using the radiotap header in MADWIFI driver [1]. The average value of the RSS of each link are used as inputs for the experiments.

In the experiments, all nodes have the same total number of radios varying between 1 and 2, and the same number of total orthogonal channels varying from 1 to 4. The minimum and maximum power levels are 1 dBm and 15dBm respectively. Twenty set of link bandwidth vectors are randomly generated as inputs, and the final results show both the average value and standard deviation for all experiments.

B. Numerical results

We first evaluate the interference margin obtained from the three algorithms. Since the SP algorithm does not generate interference margins and link rate vector itself, we take the link transmit power, radio-channel assignment results of the algorithm as inputs to our algorithm to compute these values skipping the power and radio-channel assignment steps.

Fig. 3 shows the interference margin obtained by three algorithms with different of radios (1 to 2) and channels (1 to 4). The dashed lines correspond to the results with one radio($R=1$), the solid lines correspond to the results with two radios($R=2$). The interference margin is computed as the minimum value among all links in the same setting on all experiments. As expected, when the number of radios and channels increases, the interference margin attainable by all schemes increases. However, the increments tend to flatten out for more radios and channels. The RP algorithm outperforms other two schemes in providing larger interference margin. The performance gain of RP algorithm over FP algorithm is more prominent with small number of channels. This is because RP algorithm can reduce the contention and improve the spatial reuse by optimizing the transmit power level. The performance gap between RP and FP algorithm decreases as the number of channel increases, which suggests that both algorithms can take advantage of channel assignment for improving the spatial reuse, the contribution of power control is not dominate in these cases. The performance of SP algorithm is the worst because it is agnostic to link bandwidth requirement, and it does not optimize transmit power and channel assignment jointly.

Note that the power control and radio-channel assignment decision of these algorithm is made based on the average RSS values on all links. It is interesting to study the impact of short-term channel variation on the performance of these three algorithms. In the second set of experiments, a large number of RSS samples are generated for each

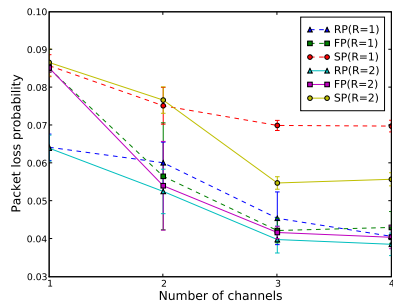


Fig. 6. Loss prob. with no interference sources

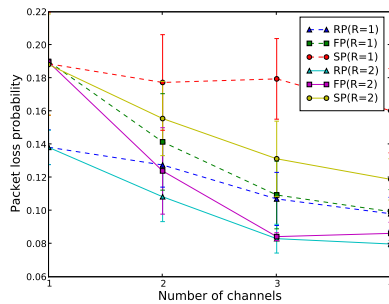


Fig. 7. Loss prob. with random interference sources

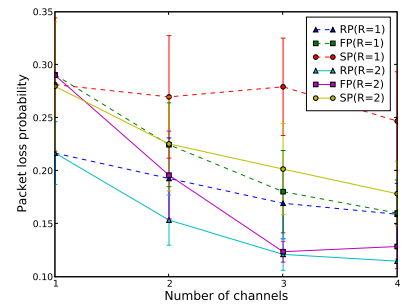


Fig. 8. Loss prob. with persistent interference sources

link using its RSS CDF profile. For each set of RSS values, we compute the SINR for each individual links and obtain their achievable transmit rates, with which we can check the radio and contention constraint (8) for each link. An *outage* occurs if this constraint is violated, and we define the *outage probability* as the percentage of violated constraints. This procedure is repeated 1000 times. The outage probability obtained by for these three algorithms is shown in Fig. 4. We see that that RP algorithm incurs less outage probability than other two algorithms under most cases, in particular with smaller number of channels. Although our algorithm does not explicitly optimize for the outage probability (which is dependent on RSS variation over time), a larger interference margin generally provides higher allowance to link variability. This is consistent with our intuition. It can also be observed from these figures that the outage probabilities are significantly reduced when more radios and channels are employed.

Fig. 5 shows the convergence behavior of the proposed algorithm for the case of 2 radios, 4 channels. In the figure, the upper bound returned by the master problem decreases monotonically and converges to the lower bound obtained from the primal problem. Optimality is obtained at around 50 iterations.

C. Simulation results

In this section, we compare the performance of the algorithms using the Qualnet simulator [27]. We choose Qualnet because it provides a PATHLOSS-MATRIX propagation model which incorporates a three-dimensional matrix indexed by source node, destination node, and time to calculate path loss between nodes. The same topology as the testbed is used in the simulations. The TDMA MAC protocol in Qualnet is modified to allow transmission of multiple packets within a slot. The TDMA schedule is generated using the algorithm discussed in Section V and imported to the simulation. Since 802.11a PHY only supports 8 transmission rates (6, 9, 12, 18, 24, 36, 48, 54Mbps), link rates obtained from the three algorithms are rounded to the next higher rate level supported by 802.11a and remain fixed throughout the simulation runs.

To study the effects of external interference, we introduce four interference sources located in the four corners of the testbed, each source can inject AWGN signals at -30dBm. We consider three scenarios for the activities of these interference sources:

- *No interference* – None of these interference sources is activated during the simulation.
- *Random interference* – Only one of the randomly selected interference sources is activated in each time slot.
- *Persistent interference* – All interference sources are activated during the simulation.

Fig. 6 shows the packet loss probability obtained by three algorithms for the case that no interference source is activated. In this case, packet losses are mainly due to the channel variations. We see that RP algorithm incurs less packet losses than other two algorithms under most cases. This is consistent with the numerical results.

Fig. 7 and 8 show the results for random and persistent interference cases respectively. As expected, due to the existence of external interference and channel variation, the packet loss probabilities are higher than the previous experiments. It can be seen from these figures that the RP algorithm achieves better performance than the other two schemes. This demonstrates that the proposed algorithm is more robust to channel variations and external interference than other schemes.

VII. CONCLUSIONS

We present an optimal joint power control and radio-channel assignment scheme for robust traffic engineering in multi-radio multi-channel(MR-MC) wireless networks. The objective is two folded i) to support link bandwidth requirements, and ii) to be resilient to moderate channel variations or external interferences. Both numerical and simulation results show that the proposed algorithm outperforms existing schemes in providing larger interference margin, and reducing outage and packet loss probabilities.

REFERENCES

- [1] MADWIFI, Multiband Atheros Driver for WiFi. <http://madwifi.org/>.
- [2] V. A., L. S., and G. I.E. Modeling of discrete/continuous optimization problems: Characterization and formulation of disjunctions and their relaxations. *Computers and Chemical Engineering*, 27(3):433–448, 2003.
- [3] M. Alicherry, R. Bhatia, and L. E. Li. Joint channel assignment and routing for throughput optimization in multi-radio wireless mesh networks. In *MobiCom '05*, pages 58–72, 2005.
- [4] S. Boyd, S.-J. Kim, L. Vandenberghe, and A. Hassibi. A tutorial on geometric programming. *Optimization and Engineering*, 8:67–127, 2007.
- [5] I. Broustis, K. Papagiannaki, S. V. Krishnamurthy, M. Faloutsos, and V. Mhatre. MDG: measurement-driven guidelines for 802.11 WLAN design. In *MobiCom '07*, pages 254–265, 2007.
- [6] P. Chaporkar, K. Kar, X. Luo, and S. Sarkar. Throughput and fairness guarantees through maximal scheduling in wireless networks. *IEEE Trans. on Information Theory*, 54(2):572–594, 2008.
- [7] G. Cote and M. A. Laughton. Large-scale mixed integer programming: Benders-type heuristics. *European Journal of Operational Research*, 16(3):327–333, June 1984.
- [8] F. F. Digham. Joint power and channel allocation for cognitive radios. In *IEEE WCNC'08*, pages 882–887, March 31 2008–April 3 2008.
- [9] G. J. Foschini and Z. Miljanic. Distributed autonomous wireless channel assignment algorithm with power control. *IEEE Trans. on Vehicular Technology*, 44(3):420–429, Aug. 1995.
- [10] Y. Gao, J. C. Hou, and H. Nguyen. Topology control for maintaining network connectivity and maximizing network capacity under the physical model. In *IEEE INFOCOM'08*, pages 1013–1021, 2008.
- [11] A. M. Geoffrion. Generalized benders decomposition. *Journal of Optimization Theory and Applications*, 10(4):237–260, 1972.
- [12] GLPK . (GNU Linear Programming Kit). <http://www.gnu.org/software/glpk/>.
- [13] C. Hua, S. Wei, and R. Zheng. Robust channel assignment for link-level resource provision in multi-radio multi-channel wireless networks. In *IEEE ICNP*, 2008.
- [14] B. Kauffmann, F. Baccelli, A. Chaintreau, V. Mhatre, K. Papagiannaki, and C. Diot. Measurement-based self organization of interfering 802.11 wireless access networks. In *INFOCOM 2007*, pages 1451–1459, 2007.
- [15] M. Kodialam and T. Nandagopal. Characterizing the capacity region in multi-radio multi-channel wireless mesh networks. In *MobiCom '05*, pages 73–87, 2005.
- [16] D. Li and X. Sun. *Nonlinear Integer Programming*. Springer, 2006.
- [17] N. Li and J. Hou. Topology control in heterogeneous wireless networks: problems and solutions. In *Proc. of IEEE Infocom 2004*, March 2004.
- [18] N. Li, J. C. Hou, and L. Sha. Design and analysis of an MST-based topology control algorithm. In *Proc. IEEE INFOCOM 2003*, San Francisco, California, US, Apr. 2003.
- [19] X.-Y. Li, G. Calinescu, and P.-J. Wan. Distributed construction of planar spanner and routing for ad hoc networks. In *Proc. IEEE INFOCOM 2002*, June 2002.
- [20] V. Mhatre, K. Papagiannaki, and F. Baccelli. Interference mitigation through power control in high density 802.11 WLANs. In *IEEE INFOCOM*, 2007.
- [21] S. Narayanaswamy, V. Kawadia, R. S. Sreenivas, and P. R. Kumar. Power control in ad hoc networks : Theory, architecture, algorithm and implementation of the COMPOW protocol. In *European Wireless Conference*, 2002.
- [22] A. Rad and V. Wong. Joint channel allocation, interface assignment and mac design for multi-channel wireless mesh networks. *IEEE INFOCOM'07*, pages 1469–1477, May 2007.
- [23] B. Radunovic and J.-Y. Le Boudec. Rate performance objectives of multihop wireless networks. *IEEE INFOCOM'04*, 3:1916–1927 vol.3, March 2004.
- [24] A. Raniwala, K. Gopalan, and T. Chiueh. Centralized channel assignment and routing algorithms for multi-channel wireless mesh networks. *SIGMOBILE Mob. Comput. Commun. Rev.*, 8(2):50–65, 2004.
- [25] E. Rozner, Y. Mehta, A. Akella, and L. Qiu. Traffic-aware channel assignment in enterprise wireless LANs. In *Proc. of ICNP*, 2007.
- [26] Scalable Network Technologies . Qualnet network simulation software. <http://www.scalable-networks.com/>.
- [27] I. Scalable Network Technologies. *QualNet 4.0 Programmer's Guide*. Scalable Network Technologies, Inc., 2007.
- [28] A. P. Subramanian, H. Gupta, and S. R. Das. Minimum interference channel assignment in multi-radio wireless mesh networks. In *IEEE SECON '07*, pages 481–490, 2007.
- [29] M. Thomas and W. Roger. The complexity of connectivity in wireless networks. In *IEEE INFOCOM*, 2006.
- [30] M. Thomas, W. Roger, and Z. Aaron. Topology control meets sinr:: the scheduling complexity of arbitrary topologies. In *MobiHoc*, pages 310–321, Florence, Italy, 2006. ACM Press.
- [31] R. Wattenhofer, L. Li, P. Bahl, and Y.-M. Wang. Distributed topology control for power efficient operation in multihop wireless ad hoc networks. In *Proc. of IEEE INFOCOM*, 2001.

- [32] X. Wu, R. Srikant, and J. R. Perkins. Scheduling efficiency of distributed greedy scheduling algorithms in wireless networks. *Trans. on Mobile Computing*, 6(6):595–605, June 2007.